Bull.Fac.Sci.Alex.Univ.,2003/2004, Vol. 43, No.1,2, pp. 119-144

THE LIPT ALKALI GRANITE PLUTON, KINGDOM OF SAUDI ARABIA: GEOCHEMICAL AND SR-ND ISOTOPIC INFERENCES ON THE PETROGENESIS OF A RARE METAL-BEARING A-TYPE GRANITE

HASSANEN M. A. AND QAHDI T. M.

King Abdulaziz University, Faculty of Earth Sciences, Department of Mineral Resources and Rocks, Jeddah, KSA.

(Received 16 April 2003, revised and accepted 25 February 2004)

Abstract. The Lipt granite pluton, northern Asir terrain, Kingdom of Saudi Arabia intrudes a deformed syn-tectonic metavolcano-sedimentary association and I-type granodiorite intrusions emplaced at about 667 ± 6 Ma. The Lipt granite pluton is composed of monzogranite, muscovite granite, porphyritic albite granite, and arfvedsonite-aegirine albite granite. Field observations strongly suggest a comagmatic origin of these granite varieties. Major, trace, REEs and Sr-Nd isotope data, indicate that the rocks of the Lipt pluton are highly fractionated specialized peralkaline A-type granite with markedly enriched in rare metals (Sn, Nb, Ta, Y, Zr and REE). Whole rock Rb-Sr dating gives ages of 559 ± 19 Ma for the monzogranite and 556 ± 7 Ma for the porphyritic albite granite. They have initial $^{87}Sr/^{86}Sr$ ratio of 0.708 – 0.709 and relatively low positive ε_{Nd} values (+0.39 - +1.06). These isotopic data indicate that the peralkaline Lipt granites can be regarded as a mixture of old crustal and juvenile mantle-derived materials. The Nd model ages for the albite granite are mostly in the range 0.98-1.3 Ga suggesting that the old crustal component is of a Middle Proterozoic age. Fractional crystallization, involving fluorine complexing and fluid fractionation, played an important role in the evolution of the Lipt granite pluton and the associated mineralizations.

1. INTRODUCTION

Although Early to Middle Proterozoic rocks have been found in the eastern part of the Arabian Shield (Stacey and Hedge, 1984), the main geologic evolution of the Shield is limited to a period ranging from 900 to 530 Ma that led to the formation, amalgamation, and final cratonization of several tectono-stratigraphic terranes. This time span has been classified into three stages (Genna *et al.*, 2002). The first (pre-Pan-African) is the 900-690 Ma time span during which Saudi Arabia was an area of mostly volcano-sedimentary formations deposited in an oceanic or marginal marine environment associated with subduction zones, and intruded by granite and diorite. Volcanic arcs and ophiolitic assemblages typical of a subduction context indicate that convergence occurred in an oceanic environment (Camp, 1984; Laval and Le Bel, 1986; Pallister *et al.*, 1987). These are represented by various groups, the main ones being the Al Ays, Abt, Halaban, Jiddah, Bahah, Baish, and Hali groups. (e.g. Hadley and Schmidt, 1980; Jackson and Ramsay, 1980). The second (Pan-African) is the 690–590 Ma time span, which was marked by the formation of the Nabitah Belt (Genna *et al.*, 2002) and various sedimentary formations represented by foreland or intracontinental molasse basins. The third stage (590–530 Ma) termed post-Pan-African and was characterized by widespread extension, which brought

about crustal thinning that generated bimodal magmatism and significant dike swarms; associated volcanics form the Shammar group.

Voluminous alkaline/peralkaline granites were emplaced during the post-collision event (590 530 Ma) in the Arabian Shield (Harris, 1985) and formed an essential crustal component of the Shield rocks (Fig. 1). Recently, post-collisional granites have drawn attention because many plutons, known as specialized granites, are typically associated with high concentrations of rare metals such as Sn, W, U, Th, REE, Be, Nb, Ta, and Mo (Ramsay, 1986; Du Bray, 1986). Knowledge of the processes involved in the generation and evolution of the specialized granites are essential for understanding the tectonic evolution of the Arabian Shield, and also for the formation of metallic ore deposits. Moreover, recent Sr–Nd isotope compilation on granites from the East African Orogen, including the Arabian Shield, revealed that most of them have Neoproterozoic Sm–Nd depleted mantle model ages and are characterized by positive $\varepsilon_{Nd}(T)$ values (Stern, 2002). This suggests that the bulk of these granites represent a significant addition of mantle material (juvenile component) to the continental crust. This paper presents elemental abundance and Sr–Nd isotopic data for the interesting Lipt granite pluton in the northern Asir terrain. The pluton consists of three granite types, namely granodiorite, monzogranite and albite granite which contains abundant rare-metal minerals such as zircon, thorite, columbite-tantalite. The aim is to examine the problem of the genesis of this rare metal bearing granite using trace element and isotopic arguments, and field relationships as well.

2. GEOLOGICAL SETTING

2.1. General setting of the Lipt area

The Jabal Lipt district lies in the extreme northern part of the Asir terrain at about 10 km north of the Bishah town and about 450 km southeast of Jeddah (Fig. 1). It lies in the northern part of the Jabal Al Hasir quadrangle (Sheet 19F, international index NE-38-1; Greenwood et al., 1986). The regional geology of the area around Jabal Lipt is shown in Fig. 2. The Precambrian rocks are mainly represented by four lithostratigraphic units (Greenwood *et al.*, 1986): 1) Highly folded and metamorphosed volcano-sedimentary association of immature epiclastic and volcaniclastic sediments (Bahah Group), mafic to felsic lavas and metasediments (Jeddah Group) and metamorphosed mafic to intermediate volcanic rocks and immature volcanogenic sediments (Halaban Group). The rocks of the three groups are components of ensimatic volcanic arc complex that have been developed during the time span 910-720 Ma (Greenwood *et al.*, 1982; Roobol *et al.*, 1983). 2) Mafic to intermediate intrusive rocks of metagabbro-diorite-tonalite forming part of the An Nimas batholith, which extends to the southern and western parts beyond the limits of the map area. The rocks of the An Nimas batholith are dated 837 – 816 Ma (Cooper *et al.*, 1979; Fleck *et al.*, 1980). 3) Foliated to gneissic granodiorite and monzogranites, which have been formed during two phases between 732-723 Ma

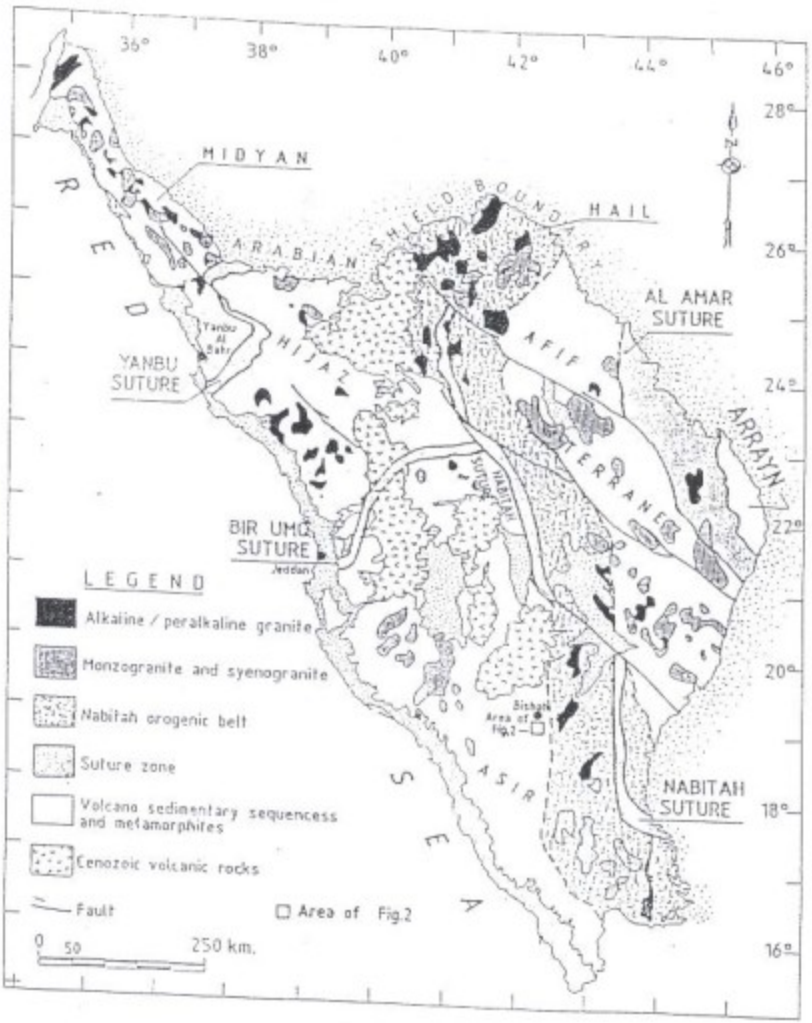

Fig. (1). A map showing location of Jabal Lipt area and distribution of granitic plutons in the Arabian Shield (modified from Ramsay, 1986)

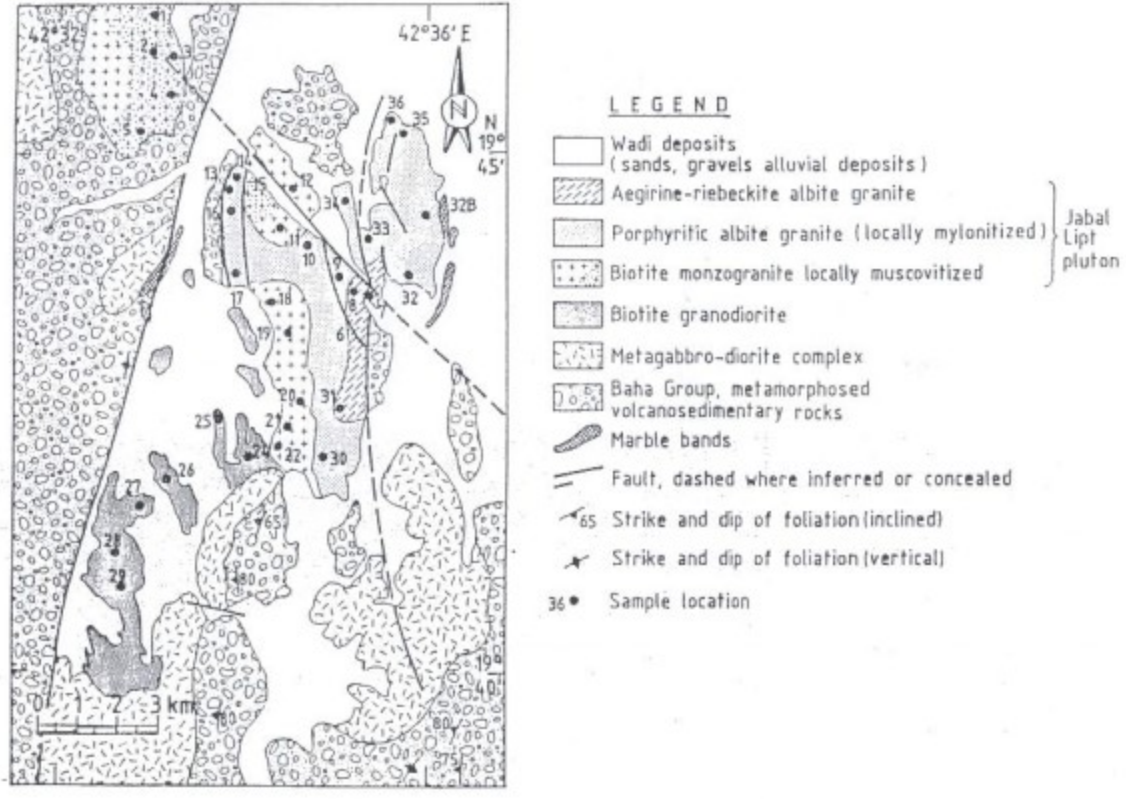

Fig. (2). Simplified geologic map of Jabal Lipt area.

and 680-640 Ma (Stoeser *et al.*, 1984). 4) Post-tectonic (630 – 530 Ma) undeformed syenite, granodiorite, monzogranite, and alkali granites. The Jabal Lipt is one of these late- to post-tectonic granite intrusions.

2.2. Geology of the Lipt granite pluton

The Jabal Lipt pluton is a N-S elongated body of about 10 km long. It was intruded into the volcano-sedimentary association of the Bahah Group and the foliated and gneissose granodiorite with sharp contacts that are locally faulted. The Lipt pluton occurs along the Rawashan fault zone and is dissected by many shear zones and faults (Fig. 2) trending NW and due N. Detailed fieldwork and petrographic studies allow distinguishing four granite types namely: 1) porphyritic monzogranite locally greisenized, 2) muscovite granite, 3) porphyritic albite granite locally mylonitized, and 4) aegirine riebeckite albite granite.

The porphyritic monzogranite is fine- to medium-grained, massive with pink to reddish pink colour and constitutes the major part of the Jabal Lipt. Angular xenoliths of volcanic and dioritic rocks are common in the monzogranite. Pervasive muscovitization and greisenization locally affected the monzogranite, where large pockets of greisenized granites are recorded. The porphyritic albite granite occupies the eastern part of the pluton and is fine- to medium-grained rock that is locally foliated, especially along major faults. A major part of the porphyritic albite granite contains abundant irregular black patches that impart a black colour to the rocks in the field. The black spots vary in diameter from few mm up to 1 m. The contact between the monzogranite and the albite granite is sharp and dips 45°S. The aegirine riebeckite albite granite occupies the eastern part of Jabal Lipt. The rock is fine-to medium-grained and has gradational contact with the porphyritic albite granite.

3. PETROGRAPHY

3.1. Granodiorite suite

The granodiorite rocks, which frequently grade into nonzogranite, are heterogeneous, medium- to coarse-grained and show subsolvus porphyritic texture with phenocrysts up to 3 cm long. The rocks consist of K-feldspar, plagioclase feldspar, quartz, biotite and minor hornblende. Titanite, apatite, zircon, magnetite are accessory minerals. Secondary minerals include chlorite, muscovite, epidote and clay minerals. K-feldspars are dominated by microcline and less common flame and mesoperthites. The microcline crystals are subhedral and show wide variation in grain size (1 mm up to 3 cm long). Plagioclase feldspar is medium- to fine-grained, subhedral with lath-like shape. The plagioclase feldspar crystals have oligoclase composition (An_{15}-An_{25}), but the fine-grained crystals have a relatively more albitic composition (An_{10}-An_{15}). Quartz is medium- to coarse-grained, anhedral and moderately strained with development of andulose extinction. Biotite is the main ferromagnesium mineral occurring as fine- to medium-grained cluster aggregates and subhedral flakes. In some samples biotite is partially altered to green chlorite while in other it is altered to muscovite. Inclusions of zircon are common in biotite with abundant pleochroic haloes.

3.2. The Lipt Pluton

3.2.1. Monzogranite

The monzogranite consists mainly of alkali feldspar, quartz, plagioclase and green biotite. Accessory phases include zircon, apatite, discrete grains of columbite-tantalite, and fluorite. The alkali feldspar is usually vein- and patch-mesoperthites. Granophyric and graphic intergrowths are common in some samples. Quartz is present as large anhedral to subhedral crystals containing inclusions of perthites and zircon. Plagioclase feldspar crystals (An_{15}-An_{25}) are medium- to fine-grained with subhedral prismatic and lath-like shape. Some plagioclase crystals are normally zoned while other display oscillatory zoning with selectively sericitized core. The biotite forms subhedral flakes and occurs as interstitial clusters or as small euhedral inclusions in feldspars. It is commonly altered to chlorite and often carries inclusions of zircon and apatite. This rock unit is partially greisenized. The greisens are in the form of pockets and veins, which exhibit intercalations of several facies which are muscovite-rich, and K-feldspar-rich. Mineralization in this rock unit is mainly encountered in the greisens and is represented by some cassiterite and tantalite-columbite minerals.

3.2.2. Muscovite granite

The muscovite granite is a homogenous, medium-grained and equigranular subsolvus granite. It consists of quartz, albite, micocline, muscovite and biotite. Zircon and apatite are accessory minerals. Albite (An_5-An_{10}) is the most abundant mineral with an average mode of 40%. The albite crystals are fine- to medium-grained, and subhedral with a characteristic prismatic to lath-like habit. Quartz (30 %) is medium-grained and highly deformed with development of severe undulose extinction. Microcline forms fine- to medium-grained tabular crystals with characteristic crosshatch to spindle shape twining. Muscovite (2-5%) occurs both as primary magmatic crystals (0.5 – 2 mm long) with kinked structure and as secondary fine scales (>0.5 mm long) formed at the expense of feldspars. Biotite is less abundant and occurs as fine-grained shreds. Fluorite is a relatively abundant accessory mineral. It is anhedral and contains many inclusions of zircon and monazite surrounded by bluish violet coloured haloes.

3.2.3. Porphyritic albite granite

This rock type constitutes the main mass of Jabal Lipt. It is homogeneous, subsolvous and porphyritic. It consists essentially of quartz, albite, K-feldspar and biotite. Titanite, apatite and zircon are the common accessory minerals, whereas muscovite, chlorite and rare epidote are alteration minerals. Quartz occurs as fine -to medium -grained (0.5 mm to 5 mm) anhedral crystals with subrounded and corroded grain boundaries. The quartz crystals are highly strained with development of undulose extinction particularly the phenocrysts. Fine-grained quartz crystals commonly occur as poikilitic inclusions in the quartz phenocrysts. Albite (An_6-An_9) is fine-grained (0.2- 1 mm in diameter), subhedral with fine lath-like forms. The black patches in the albite granite consist of fine albite lathes either delineated with

brownish material containing disseminated opaques (Nb-Ta minerals) and/or filling the cleavage planes and micro fractures. The K-feldspar crystals are fine-grained (0.5- 1 mm) with anhedral form. Few large K-feldspar crystals display patch perthite, while others show thin and clear albitized rim. Some biotite crystals contain quartz and albite inclusions indicating a late magmatic crystallization of the biotite. Accessory minerals are relatively abundant, which include zircon as the most abundant one followed by apatite, titanite and discrete grains of columbite-tantalite and tapiolite.

A mylonitized albite granite variety occurs close to fault planes and is mineralogically similar to the medium-grained albite granite variety, but differs in having minor aegirine-augite and arfvedosonite and relatively more rich in accessory minerals (e.g. zircon, titanite, apatite).

3.2.4. Riebeckite-aegirine albite granite

This granite variety is porphyritic with the common development of flow texture due to the subparallel arrangement of mineral laths. It consists of albite, quartz, microcline, riebeckite, aegirine-augite and biotite. Zircon is the most abundant accessory mineral followed by apatite. Albite (An_0) constitutes the main part of the groundmass and shows a subparralel alignment imparting to the rock fluidal-like texture. Piokilitic inclusions of albite laths in the quartz phenocrysts are common. Quartz occurs both as highly strained and undulatory anhedral phenocrysts and anhedral grains in the groundmass. K-feldspar crystals are almost of microcline together with minor patch and cryptoperthites. Poikilitic inclusions of albite laths in microcline are common. Ferromagnesian minerals include alkali pyroboles (riebeckite and aegirine-augite) and biotite.

4. ANALYTICAL TECHNIQUES

Based on the petrographic investigations, 25 representative samples covering the different granite varieties were selected for major, trace and rare earth element analyses. Major element compositions and Sc, Ba, and Ni abundances were determined by inductively coupled plasma-atomic emission spectrometry (ICP-AES). The elements Mo, Cu, Pb, Zn, As and Bi were determined by ICP-AES where 0.5 gm of powdered sample was leached by 3 ml HCl-HNO_3-H_2O mixture at 95°C for one hour. The remainder of trace elements and the rare earth elements (REE) were determined by inductively coupled plasma-mass spectrometry (ICP-MS). All the analyses were carried out at the ACME Analytical Laboratories Ltd., Canada. Analytical precision, as calculated from replicate analyses, is 0.5% for major elements and varies from 2-5% for trace elements of >80 ppm, 2-10% for trace elements of 10-80 ppm, and 5-20% for trace elements of <10 ppm. The analytical data are given in Tables 1.

Table 1: of major, trace and rare earth elements contents in the Lipt area, Asir Terrain, KSA.

	Granodiorite							Monzogranite (pink granite)				
Sample N	L-16	L-24	L-25	L-26	L-27	L-28	L-29	L-6	L-9	L-10A	L-18	L-32A
SiO_2	73.79	69.68	70.64	72.34	71.00	72.19	72.39	72.52	70.92	72.35	71.93	72.47
TiO_2	0.08	0.45	0.47	0.23	0.24	0.17	0.35	0.12	0.24	0.21	0.24	0.18
Al_2O_3	13.18	14.38	14.19	14.09	14.50	14.41	13.62	14.20	13.31	13.15	13.72	13.23
Fe_2O_3	1.07	2.42	2.49	1.44	1.41	1.17	1.92	1.28	1.75	1.69	1.75	1.36
MnO	0.04	0.05	0.05	0.03	0.03	0.03	0.04	0.07	0.11	0.09	0.08	0.09
MgO	0.03	0.72	0.70	0.33	0.35	0.26	0.60	0.19	0.30	0.24	0.26	0.17
CaO	0.67	2.26	2.13	1.36	1.19	1.09	1.61	1.04	1.00	0.84	0.96	0.64
Na_2O	4.89	3.94	3.91	3.73	4.64	3.79	4.68	5.04	5.14	5.51	4.97	5.41
K_2O	6.19	4.64	4.34	5.68	5.74	6.36	4.10	4.91	6.02	5.60	5.73	5.63
P2O5	0.01	0.11	0.12	0.03	0.06	0.02	0.06	0.01	0.04	0.05	0.03	0.01
LOI	0.10	1.20	0.80	0.60	0.70	0.50	0.70	0.40	0.89	0.10	0.20	0.60
Total	100.1	99.85	99.84	99.86	99.86	99.90	99.87	99.78	99.72	99.83	99.87	99.79
Trace Elements (ppm)												
Ni	2	2	2	2	2	1	1	1	2	2	1	2
Co	2	4	5	2	3	2	4	2	3	2	2	1
Sc	1	5	4	3	2	2	1	2	5	2	5	1
V	5	22	23	5	7	5	17	5	5	5	5	5
Cu	4	3	3	2	3	7	5	7	2	3	2	4
Pb	32	6	3	4	6	8	6	45	17	30	7	39
Zn	120	66	60	41	45	31	61	67	175	129	107	119
Sn	1	3	3	3	3	4	5	15	8	3	5	8
W	66	12	43	16	7	18	1	25	34	14	1	1
Rb	118	134	141	191	206	244	160	360	216	301	164	307
Cs	0.50	3.70	6.80	5.20	5.40	9.30	6.00	10.10	4.30	2.10	3.60	3.80
Ba	27	514	488	691	662	563	506	221	369	288	336	217
Sr	16	295	313	222	221	171	272	77	105	90	69	72
Tl	0.60	0.60	0.60	0.80	0.50	1.10	1.00	1.10	0.60	0.50	0.40	0.90
Ga	33	24	24	24	26	25	27	31	30	29	30	35
Ta	0.80	0.90	1.20	1.10	1.00	1.50	1.10	8.00	2.40	2.10	2.40	2.20
Nb	6.0	7.9	7.5	6.6	6.4	7.8	8.4	34.9	29.1	20.9	19.9	34.3
Hf	2.9	5.4	6.6	5.1	4.6	3.4	5.5	6.6	8.00	8.4	6.9	9.8
Zr	91	190	235	177	147	103	179	127	235	261	229	265
Y	19	17	14	12	10	14	11	74	58	65	61	69
Th	4.0	14.5	16.9	18.1	19.4	16.8	10.8	35.2	12.40	12.1	13.5	31.7
U	2.8	4.8	5.2	7.7	3.8	8.3	4.7	17.7	6.30	4.8	6.2	6.0
La	9.6	38.1	41.3	33.7	29.7	24.1	26.8	25.6	54.7	57.6	69.2	58.8
Ce	100.6	81.2	81.0	66.8	58.8	49.3	53.5	56.0	120.2	133.0	159.6	133.8
Pr	2.40	8.94	8.83	7.33	6.72	5.66	6.16	6.90	15.45	16.11	18.97	16.44
Nd	8.4	32.7	33.1	27.0	25.8	20.1	23.4	27.0	56.90	62.8	71.7	62.4
Sm	1.80	6.00	5.20	4.90	4.30	4.70	4.30	7.20	12.20	12.90	13.50	13.00
Eu	0.41	1.20	1.13	0.87	0.78	0.67	0.81	0.52	1.37	1.43	1.49	1.30
Gd	2.00	3.87	3.75	3.24	2.93	3.04	2.70	7.65	9.67	10.65	9.85	10.46
Tb	0.30	0.57	0.50	0.39	0.38	0.47	0.39	1.38	1.49	1.73	1.63	1.65
Dy	1.74	3.26	2.72	2.16	2.01	2.57	2.00	9.31	8.53	10.66	9.30	9.79
Ho	0.37	0.57	0.51	0.43	0.32	0.48	0.44	1.98	1.72	2.09	1.95	2.13
	0.99	1.73	1.43	1.19	0.97	1.36	1.02	6.45	4.95	6.48	5.99	6.18
	0.14	0.22	0.19	0.16	0.10	0.19	0.17	1.03	0.68	0.89	0.85	0.91
	1.10	1.37	1.39	1.06	0.75	1.22	0.85	7.13	4.67	5.86	5.64	6.56
	0.16	0.28	0.22	0.18	0.12	0.18	0.16	1.22	0.74	0.94	1.01	1.14
K/Rb	436	287	255	243	231	216	213	113	231	154	290	152
Rb/Sr	7.5	0.5	0.5	0.9	0.9	1.4	0.6	4.7	2.1	3.3	2.4	4.3

* = Total iron as Fe2O3

Isotopic ratios of Sr and Nd and the concentrations of Rb, Sr, Sm and Nd in 15 samples of the Lipt granite pluton are determined by isotope dilution at the Geology Department, Bergen University, Norway, using a VG 354 and Finnigan MAT 262 mass spectrometers. The $^{87}Sr/^{86}Sr$ and $^{143}Nd/^{144}Nd$ ratios were normalized within-runs to $^{86}Sr/^{87}Sr=0.1194$ and to $^{146}Nd/^{144}Nd = 0.7219$. Laboratory values for standards at the time of running the samples were: Johanson and Matthey (JM) Nd2O3, batch no. S819093A yielded $^{143}Nd/^{144}Nd=0.511101 \pm 15$ (2σ), NBS 987 yelded $^{87}Sr/^{86}Sr = 0.71015 \pm 4$ (2σ). The decay constant used for ^{87}Rb is $1.42x10^{-11}$ and for ^{147}Sm is $6.54x10^{-12}y^{-1}$. Initial $^{143}Nd/^{144}Nd$ and $^{87}Sr/^{86}Sr$ were calculated for individual samples at the time of crystallization and are expressed in εNd and εSr using present-day $^{147}Sm/^{144}Nd=0.1967$; $^{143}Nd/^{144}Nd =0.512638$; $^{87}Rb/^{86}Sr=0.7045$ (Allegre *et al.*, 1983; Jacobsen and Wasserberg, 1984). The age calculations have been carried out using the Isoplot 2.57 software package (Ludwig, 1991), using model 3 for regressions with elevated mean square of the weighted deviations (MSWD). If the MSWD exceed the F-variate (McIntyre *et al.*, 1966), the regression was deemed an errorchron and errors for ages and initials were multiplied by $MSWD^{1/2}$. All uncertainties are 2 sigma and errors are given at 95% confidence limits. Model Nd ages (T_{DM}) were calculated according to the depleted mantle model of DePaolo (1981)

5. GEOCHEMISTRY

5.1. Major and trace elements variations

The SiO_2 contents for the rocks of the Lipt granites range from 69 to 77 %. According to petrography and major and trace elements composition, two rock-groups can be distinguished in the pluton; these are granodiorite suite and the Lipt granite pluton (monzogranite, muscovite granite and albite granite). The granodiorites are the least evolved rocks (SiO_2 = 69.7 - 73.8%) and are medium- to low-Ca granites (CaO = 0.7 - 2.3%) with high K_2O (4.1 - 6.4%), $K_2O/Na_2O > 1$, K/Rb ratio = 213 – 435 and Rb/Sr = 0.4 – 7.4 (Table 1). The monzogranites of the Lipt pluton are relatively more evolved (SiO_2 = 71 - 72.5, CaO = 0.6 – 1%, K/Rb = 113 – 290, Rb/Sr = 2.4 – 12.3). They have lower Al_2O_3, TiO_2, MgO, CaO, Ba and Sr but have higher Rb, Y, Nb, Sn, Ta, Hf, Th, U, and REE than the granodiorites (Table 1). The muscovite granite and the albite granite resemble the monzogranites but have lower CaO, TiO_2, Sr, Ba and higher Na_2O, Rb, Zr, Nb, Sn, Ta, Hf, Th, U, and REE (Table 1). The K/Rb ratios in the muscovite and albite granites are uniformly low (55 - 176) whereas the Rb/Sr ratios (6 – 53) are high. The high Na_2O contents (4.2 - 7.4%) in the albite granite reflect the common presence of albite. The variations of some major and trace elements (Fig. 3) show a gradual decrease in Al_2O_3, CaO, Na_2O+K_2O, Ba, and Sr with increasing SiO_2 in the various granitic varieties of the Lipt pluton. Ta and Nb display very wide variations over a restricted range of silica.

Primitive mantle normalized plots of the studied granites are shown in Fig. 4. Normalized spider-diagrams of the granodiorite (Fig. 4a) display LILE-enrichment relative to HFSE and show relatively weak Sr, and Ti negative anomalies. These anomalies may be related to the fractionation of plagioclase (Sr), and/or Fe-Ti

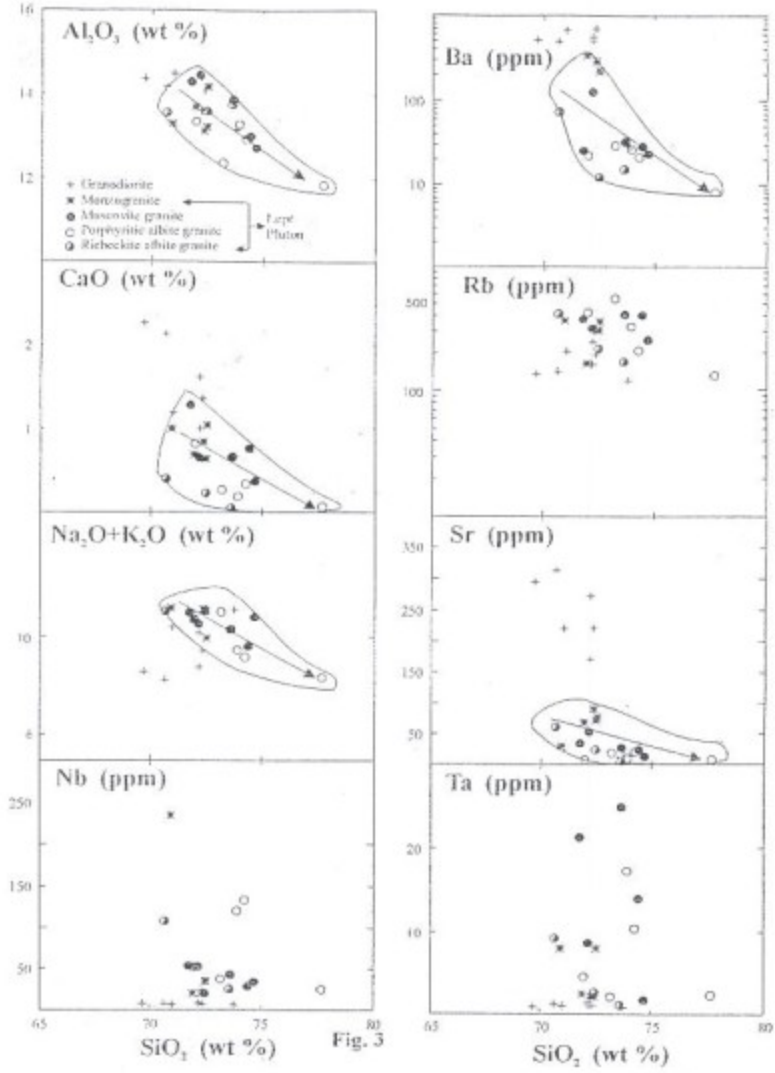

Fig. 3

Fig. (3). Harker's variation diagrams of some major and trace elements of the Lipt granites.

oxides (Ti). Distinctive depletion in Nb is a characteristic feature of arc granitoids. The monzogranites show patterns very similar to the granodiorite suite but with more obvious Ba, Nb, Sr and Ti negative anomalies (Fig. 4b), a feature similar to syn-orogenic calc-alkaline granitoids and contrasts with anorogenic alkaline granitoids. However, they share the enrichment of HFSE and depletion of Sr, Ba, Eu and Ti with the anorogenic alkaline granites. On the other hand, the muscovite and albite granites share all the compositional characteristics with the anorogenic alkaline granites being enriched in HFSE (Nb, Zr, Hf, Ta, and REE) and strongly depleted in Ba, Sr, and Ti (Fig. 4c,d).

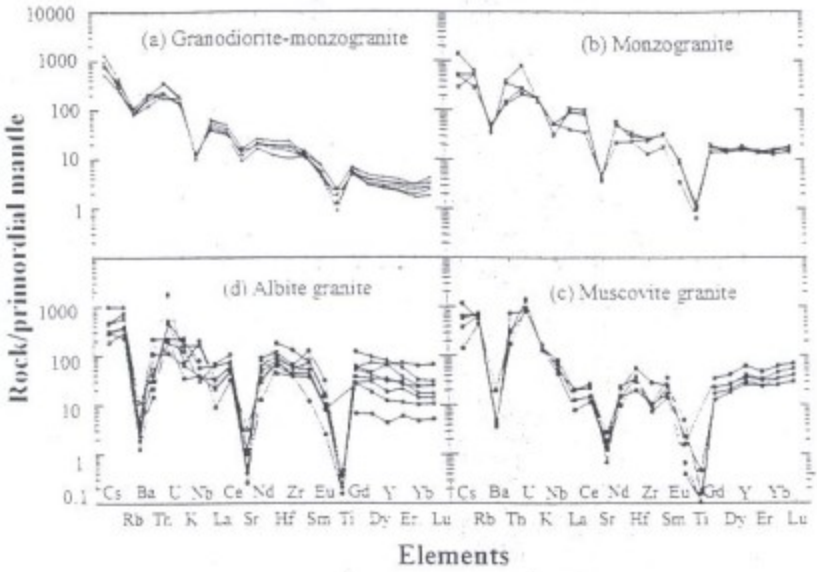

Fig. (4). Primitive mantle-normalized multi-element diagrams for the Lipt granites Normalizing values are from Sun and McDonough (1989).

5.2. Rare earth elements

Chondrite-normalized REE patterns of the different granite varieties are presented in Fig. 5. The granodiorites are enriched in LREE relative to HREE (La_n/Yb_n ratios = 5.9 –27), moderately fractionated HREE (Gd_n/Yb_n=1.5 – 3.2) and possess small negative Eu anomalies (Eu/Eu*= 0.5 – 0.7). The three rock types of the Lipt pluton show slight differences in the degree of LREE and HREE fractionation patterns. However, there is a pronounced increase in the HREE and in the depth of the Eu-anomalies from the monzogranite to the albite granite. The REE patterns of the monzogranites have a moderate Eu anomaly (Eu/Eu*= 0.2 - 0.5), nearly flat HREE

($Gd_n/Yb_n \approx 1$) and moderately fractionated LREE patterns (La_n/Sm_n ratios = 2.2 - 3.2). Compared to the monzogranite, the muscovite granite is enriched in HREE relative to LREE (La_n/Yb_n (0.2 – 0.7) and possess much deeper negative Eu anomaly (Eu/Eu* = 0.2 – 0.04). The albite granites are characterized by nearly flat REE patterns ($La_n/Yb_n \approx 1$) and a deep Eu anomaly (Eu/Eu*= 0.2 - 0.3).

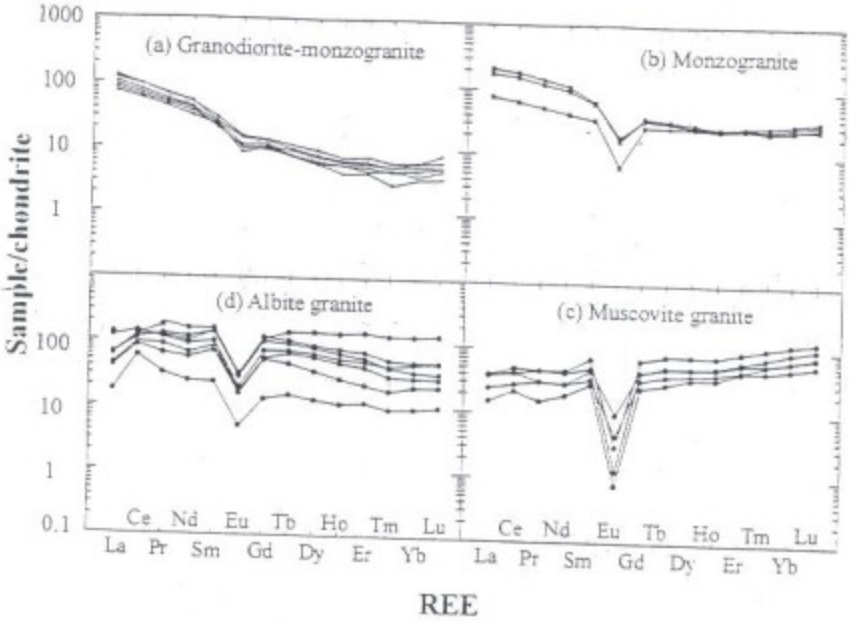

Fig. (5). Chondrite-normalized REE patterns of the Lipt granites. Normalizing values are from Sun (1982).

5.3. Magmatic affinity and tectonic setting

The granodiorite has an alumina saturation index (Al_2O_3/Na_2O+K_2O+CaO) < 1 and Al_2O_3/Na_2O+K_2O > 1 reflecting their metaluminous character (Fig. 6a). The monzogranite and the albite granite, on the other hand, are classified as peralkaline granites (Fig. 6a). The R1-R2 diagram (Fig. 6b) of de la Roche et al. (1980) with the alkaline trends from Debon and Lemmet (1999) shows that the monzogranite and the albite granite samples are classified as anorogenic alkali granites. The granodiorite samples lie in the field of calc-alkaline late-orogenic granites (Fig. 6b). Rb, Nb and Y, among other trace elements, have been used to discriminate between different tectonic settings of granitoid rocks (Pearce et al. 1984). The granodiorite is classified as volcanic arc granite, whereas the monzogranite and the albite granites are more enriched in Nb+Y and plot in the field of within-plate granite on the

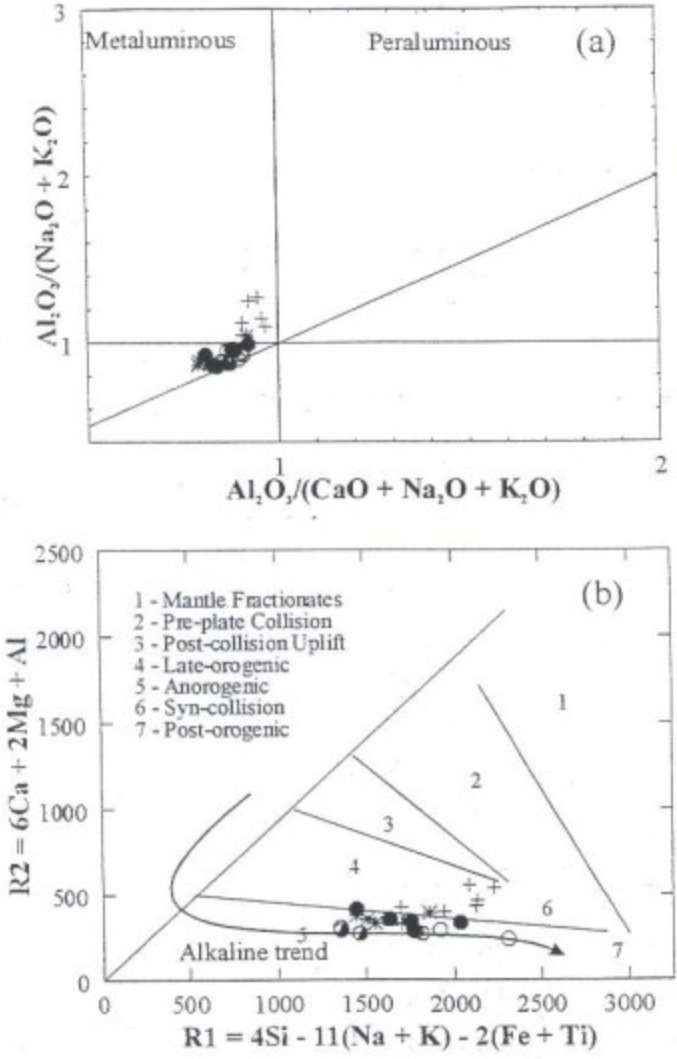

Fig. (6). Major and trace element characteristics and chemical classification diagrams for the Lipt granites, (a) $Al_2O_3/CaO+Na_2O+K_2O$ vs. Al_2O_3/Na_2O+K_2O (Maniar and Piccoli, 1989; Shand, 1927), (b) R1-R2 diagram (de la Roche et al. 1980) with the alkaline trend from Debon and Lemmet (1999).

tectonic discrimination diagram of Pearce et al. (1984) (Fig. 7a). On the Zr+Nb+Ce+Y versus FeO*/MgO diagram (Fig. 7b) of Whalen et al. (1987), the granodiorite is classified as fractionated I-type granite, whereas the monzogranite and the albite granite are classified as A-type granites. Eby (1990, 1992) subdivided A-type magmas into two groups: A_1, which represents differentiates of mantle-derived oceanic island basalts (anorogenic or rift zone magmas), and A_2 granites represent a much broader range of environment and include post-collisional granites and those that were emplaced at the end of a long period of granitic magmatism. Diagrams designed to discriminate between the A_1 and A_2 groups of anorogenic magmas indicate that most samples of the Lipt granites plot in the A_2 field on the Y-Nb-Ce ternary diagram (Fig. 7c) of Eby (1992). Thus, the Lipt granite pluton represents A_2 subtype granites characterizing post-collisional setting. This agrees with previous studies where granites with A-type geochemical signatures in the Arabian Nubian Shield are considered to be formed during a post-orogenic extension period commencing at about 600 Ma (Greiling *et al.*, 1994; Beyth *et al.*, 1994; Stern, 1994; Hassanen, 1997; Küster and Harms, 1998).

5.4. Sr-Nd isotope data and geochronology

The $^{87}Rb/^{86}Sr$, $^{87}Sr/^{86}Sr$, $^{147}Sm/^{144}Nd$ and $^{143}Nd/^{144}Nd$ isotopic ratios together with the ε_{Nd}, ε_{Sr} and T_{DM} values (Table 2) have been obtained for samples of the investigated Lipt granite as well as the surrounding granodiorite suite. Regression of the analyzed 5 granodiorite samples yields an isochron age of 667 ± 6 Ma, an initial $^{87}Sr/^{86}Sr$ ratio of 0.7026 ± 0.00013 and a mean of the weighted deviates (MSWD) of 0.8 (Fig. 8a). For the monzogranite, 5 samples define an isochron (MSWD = 0.6) with an age of 559 ± 19 Ma and initial $^{87}Sr/^{86}Sr$ ratio of 0.70769 ± 0.00116 (Fig. 8b). For the porphyritic albite granite, a 5 points isochron (MSWD = 1.6) yields an age of 556 ± 7 Ma with an initial $^{87}Sr/^{86}Sr$ ratio of 0.70915 ± 0.00338 (Fig. 8c).

The age and initial $^{87}Sr/^{86}Sr$ ratio of the granodiorite indicate that these rocks were mainly derived during the Pan-African orogenic event (690–590 Ma time span, Genna et al., 2002) from a juvenile source, and preclude the involvement of an old sialic crust in their genesis. The age of the monzogranite and the albite granite are very similar and reflect the time of intrusion of this granite pluton, and they are post-collision. Similar ages (590 – 518 Ma) and moderately high initial $^{87}Sr/^{86}Sr$ ratios (0.707 – 0.714) have been reported for many alkaline/peralkaline granites from the Arabian Shield (Duyverman et al., 1982; Calvez and Kemp, 1982; Calvez et al., 1983; Qhadi, 2003).

The high Initial Sr ratios of the Lipt granite pluton are compatible with old continental crust component and may reflect either complete derivation from old crust or mixing between two end members, one of them was an old crust (Pre-Pan-Afrrican crust). The calculated ε_{Nd} values show restricted variation from +0.39 to 0.56 while ε_{Sr} display relatively wide range from +15 to –54 (Table 2). The correlation between ε_{Nd} and ε_{Sr} values shows a horizontal trend with a narrow range of ε_{Nd}. This horizontal trend is similar to that displayed by the Um Al Birak peralkaline granites in the Arabian Shield (Qhadi, 2003) and peralkaline extrusive rocks from Socorro Island (Bohrson and Reid, 1997). The positive and low ε_{Nd} values for the Lipt albite granite provide good evidence for mantle-derived and old

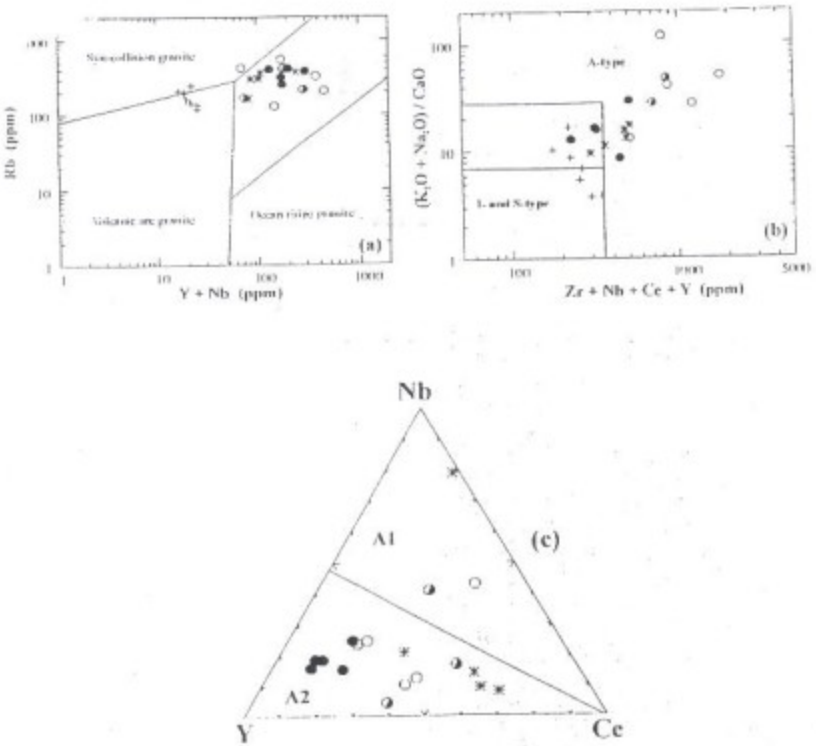

Fig. (7). Tectonic discrimination diagrams for the Lipt granites. (a) Rb vs. Y+Nb diagram (Pearce *et al.*, 1984), (b) Na_2O+K_2O/CaO vs. Zr+Nb+Ce+Y diagram (Whalen et al., 1987), (c) Y-Nb-Ce bternary diagram (Eby, 1992). Symbols as in Fig. 3.

Table 2: Rb-Sr and Sm-Nd data for the Lipt granitoids

Sample	Rb/Sr	$^{87}Rb/^{86}Sr$	$^{87}Sr/^{86}Sr \pm 2\sigma$	εSr^{t}	Sm/Nd	$^{147}Sm/^{144}Nd$	$^{143}Nd/^{144}Nd \pm 2\sigma$	εNd^{t}	T_{DM} (Ga)
Granodiorite (667 +/- 6 Ma)									
L-25	0.45	1.3061	0.714932 ± 86	-17					
L-26	0.87	2.5257	0.726698 ± 96	-15					
L-27	0.93	2.7039	0.728298 ± 64	-16					
L-28	1.43	4.1465	0.741952 ± 78	-17					
L-29	0.59	1.7114	0.718881 ± 94	-16					
Monzogranite (559 +/- 19 Ma)									
L-6	4.66	12.81	0.809001 ± 28	44					
L-10A	3.34	9.27	0.781219 ± 21	50					
L-18	2.36	6.64	0.760012 ± 19	46					
L-9B	1.89	5.51	0.752020 ± 19	41					
L-10B	4.72	13.8	0.818120 ± 22	61					
Porphyritic albite granite (556 +/- 7 Ma)									
L-9	1.89	5.51	0.752031 ± 9	64	0.199	0.1210	0.512391 ± 6	0 39	0.98
L-31A	33.55	104.92	1.536534 ± 9	15	0.232	0.1410	0.512472 ± 7	0.54	1.08
L-36	50.95	166.31	2.018268 ± 9	-54	0.271	0.1650	0.512560 ± 6	0 56	1.30
L-33	35.79	112.61	1.609808 ± 10	182	0.44	0.2680	0.512961 ± 6	1.06	
L-7	9.64	28.5	0.934588 ± 10	69	0.232	0.1410	0.513002 ± 7		

The 2 σ standard error in $^{87}Rb/^{86}Sr$ and $^{147}Sm/^{144}Nd$ is 1%. Analytical uncertainties in $^{87}Sr/^{86}Sr$ used to weight the regression and to calculate the MSWD are 0.2%.

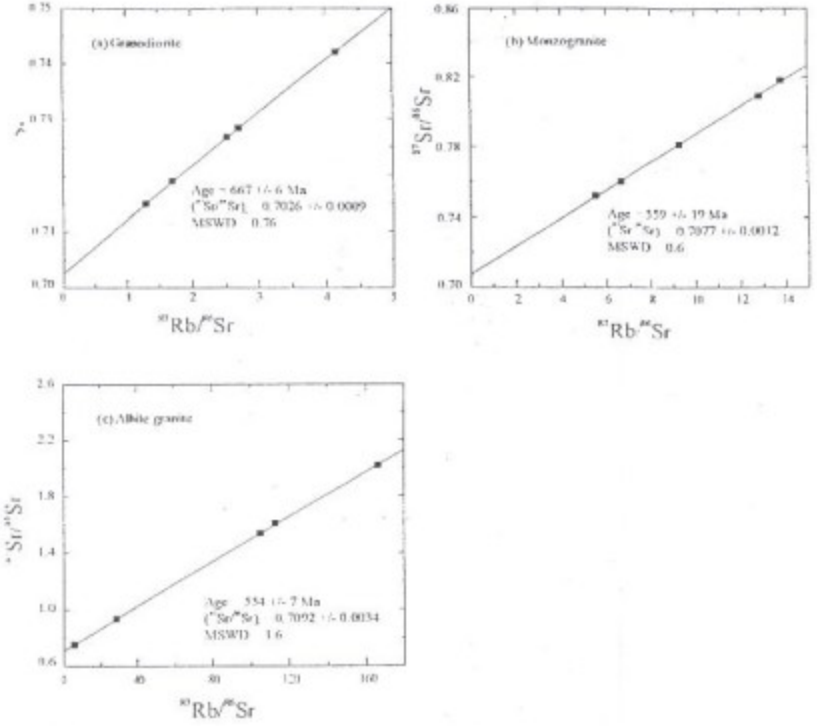

Fig. (8). Rb/Sr isochrones for the granites in the Lipt area.

crustal components. The calculated Nd model ages (T_{DM}) lie in the range 0.98 – 1.3 Ga which is higher than the crystallization age and also suggest their partial derivation from the mixing between a ca. 550 Ma mantle derived component and an old continental component which could be Middle Proterozoic crust similar to that in the Afif terrain (Stacey *et al*., 1980; Stacey and Stoeser, 1983).

6. DISCUSSION

6.1. *Petrogenesis of the granodiorite*

The granodiorite suite displays many geochemical features, including high Ba (488 - 691 ppm), Sr (171 - 313 ppm), Rb (118 - 244 ppm), Nb (6 - 8 ppm), and Th (4 - 19 ppm) indicating an enriched source rock. As mentioned before, the studied granodiorite has a composition and age (667 Ma) similar to granitoid rocks formed

during the late orogenic stage in the Arabian Shield. The low initial Sr ratio (0.07026) indicates low Rb/Sr source, which could be the mantle or juvenile crustal reservoir. During the late orogenic stage in the Arabian Shield, collision between E and W Gondwana land (Stern, 1994; Genna *et al.*, 2002) led to crustal thickening. Underplating of a mafic magma most easily occurs in such an environment and may induce partial melting in the lower crust. The composition of the crust at this stage is predominantly juvenile island arc calc-alkaline volcanic, sedimentary and plutonic materials with an average amphibolitic composition (Gettings *et al.*, 1986). Partial melting of this LILE-enriched island arc crust has been frequently invoked as an explanation for the generation of high-K granodioritic magma (Wolf and Wyllie, 1994). Based on the geochemistry of the investigated granodiorite, a largely similar petrogenetic scenario involving crustal melting of amphibolitic lower crust can be suggested. In this model, underplating of a basaltic magma and its intrusion into the crust can serve as energy-transfer mechanism that initiate partial melting in the crustal rocks to generate low-silica granitic melt (Bergantz, 1989). This melt evolved by limited fractional crystallization to produce the present granodiorite suite.

6.2. Petrogenesis of the peralkaline granite

Recent models for the petrogenesis of post-collision alkaline A-type granites (Landenberger and Collins, 1990; King *et al.*, 1997; Küster and Harms, 1998) suggest partial melting of lower crustal sources followed by fractional crystallization. Sylvester (1989) and Creaser *et al.* (1991) suggested that A-type granites may be better modelled by partial melting of an undepleted I-type tonalitic to granodioritic source. In Saudi Arabia, hornblende- and biotite-bearing I-type tonalites and granodiorites are common (Jackson, 1986) and can provide a suitable protolith for the Lipt A-type granites. However, the high initial $^{87}Sr/^{86}Sr$ ratio of the investigated granites rule out their direct derivation from Pan-African tonalites and granodiorites with initial $^{87}Sr/^{86}Sr$ ratio of 0.702 – 0.704 (Duyverman *et al.*, 1982; this study). Thus, a plausible explanation of the high initial $^{87}Sr/^{86}Sr$ (0.708 – 0.709) ratios and low ε_{Nd} values (+0.39 – +1.06) in the studied Lipt granites is their derivation by partial melting of mantle material followed by direct interaction with old continental crust beneath this region.

The Lipt granite pluton has remarkably high average concentrations of granitophile elements like Cs, Sn, Nb, Ta, Y, and Rb (Table 1), which is similar to plumasitic specialized granites in the Arabian Shield (Ramsay, 1986) and Worldwide rare metal-bearing granites (Heinrich, 1990; Raimbault *et al.*, 1990). These high concentration levels of granitophile elements make it possible to consider the Lipt albite granite as a mineralized granite. In this respect, the high Sn (>15 ppm) and Rb (>500 ppm) contents and the low K/Rb ratio (< 100) are considered as good indicators for rare-metal potential (Barsukov, 1957; Tischendorf, 1977; Ramsay 1986) where it is very low in strongly differentiated or metasomatically altered granites. In Table 1, these values in most samples of the Lipt granite pluton are within the limits of the mineralized granites.

Two principal evolutionary models have been invoked for the mineralized albite granites: 1) a magmatic model (Mackenzie *et al.*, 1988; Cuney *et al.*, 1992; Clarke *et al.*, 1993; Dostal and Chatterjee, 1995) as a result of magmatic differentiation and 2) a metasomatic model (Higgins *et al*, 1985; Nurmi and Haapala, 1986) that envisages subsolidus transformation of leucogranite to albite granites by post-magmatic hydrothermal alterations. However, the following field, petrographic and geochemical observations are serious obstacles for the metasomatic model as the main evolutionary model for the Lipt granite pluton: 1) Intrusive sharp contacts with the country rocks without albitization. 2) Gradational contact between the different albite granite varieties that means comagmatic relationship. 3) The magmatic textures and mineralogy (euhedral albite laths aligned along growth planes of quartz and K-feldspar) indicate that albite in the albite granite is an early magmatic phase. 4) Replacement textures of albite after K-feldspar (evidence of metasomatism) in the albite granite are very minor and do not agree with the percolation of large amounts of fluids through the pluton required by a metasomatic process. 5) Moody et al. (1985) have shown that oligoclase/andesine is converted to albite only below 400°C, but the presence of aegirine/augite in the Lipt albite granite indicates higher temperatures. 6) The well-defined Rb/Sr isochrons (MSWD = 0.6 – 1.6, Fig. 8) for the Lipt albite granite rule out metasomatic processes in their evolution, 7) Nb and Ta may be highly enriched during metasomatic albitization, but do not vary regularly with the degree of albitization (Wedepohl, 1971). The positive correlation between Nb and Ta (Fig. 9a) and the limited variation of Ta/Nb ratio in most samples with increasing Na_2O (Fig. 9b) indicate that the behaviour and enrichment in Nb and Ta are not related to albitization processes.

Moreover, similar to many rare-metal-bearing granites (Groves, 1972; Sheraton and Black, 1973), the analyses of the Lipt albite granite are strongly biased toward the Rb apex (strongly differentiated granites) on the Rb-Ba-Sr diagram (Fig. 10) of El Bouseily and El Sokkary (1975). These geochemical data reveal that the Lipt granite pluton has evolved by means of fractional crystallization. However, fractional crystallization alone cannot explain the very high abundances of HFSE and REE. The effects of fluorine in granites is well known (Manning, 1981) and it is suggested that F-rich fluids could produce HREE and HFSE enrichment in the late stages of evolution of granitic melt due to F complexing (Dingwell, 1988; Rogers and Satterfield, 1994). In the studied granites, there are abundant field and geochemical evidence of the presence of a late magmatic fluid phase. Field evidence includes the presence of greisen pockets and veins associated with rare metal mineralization as well as fluorite, which occur as common interstitial phases.

To conclude, fractional crystallization plays a significant role during the evolution of the Lipt granite pluton. Additional and complementary processes such as fluorine complexing and fluid fractionation contribute to the ultimate composition and specialization of the Lipt granite pluton

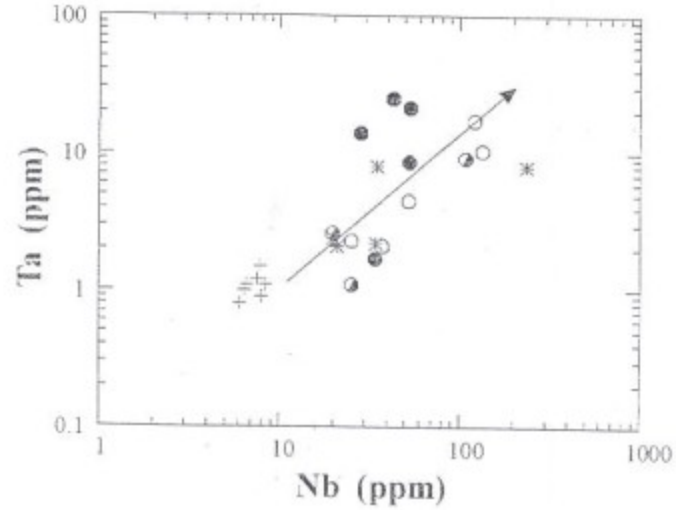

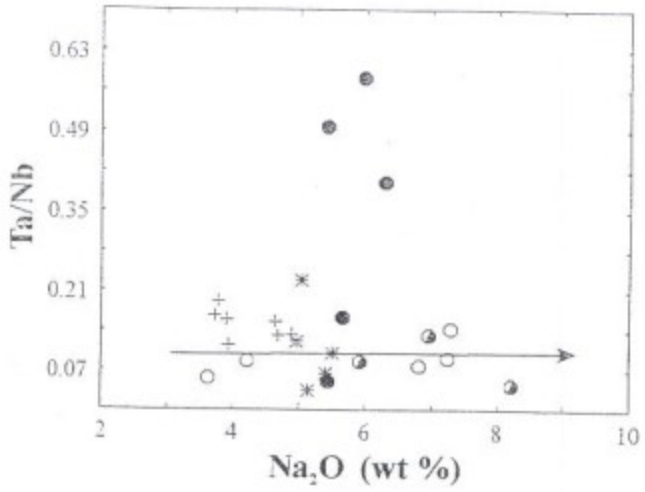

Fig. (9). The binary variation of (a) Ta vs. Nb and (b) Na_2O vs. Ta/Nb in the Lipt granites. Symbols as in Fig. 3.

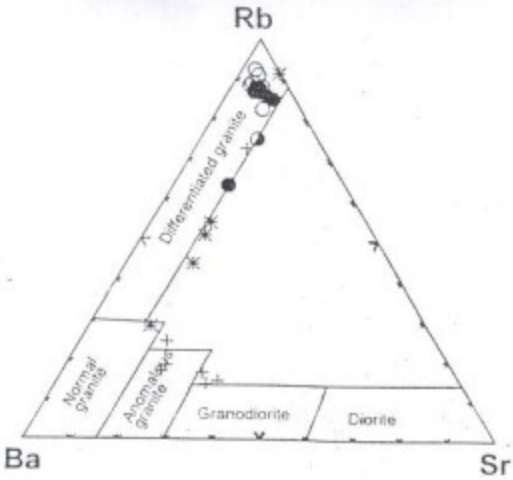

Fig. (10). Sr-Ba-Rb ternary diagram (El Bouseily and El Sokkaary, 1975) for the Lipt granites. Symbols as in Fig. 3.

7. CONCLUSIONS

The data presented here lead to the following concluding remarks:

1. The Lipt granite pluton is an example of post-collision A-type alkaline granite. The pluton consists of four granitic types: subsolvus monzogranite, muscovite granite, porphyritic albite granite and aegirine-arfvedosonite albite granite.
2. Field relations, textural characteristics and geochemical relationships argue for a comagmatic continuous evolution of the three granite varieties. The quartz in the albite granite contains many minute euhedral albite laths which indicate early crystallization of albite according to the criteria of Schwartz (1992). The granite is also associated with greisen pockets and veins, which are composed mainly of annite-like biotite together with small amounts of fluorite, cassiterite, and tantalite-columbite.
3. The I-type granodiorite was emplaced at about 667 ± 6 Ma and displays low $^{87}Sr/^{86}Sr$ initial ratio (0.7026), which suggests production by partial melting of juvenile lower crustal sources.
4. Whole rock Rb-Sr dating indicates ages in the range of 559 ± 19 Ma and 556 ± 7 Ma for the Lipt granite pluton with $^{87}Sr/^{86}Sr$ initial ratio of 0.708 – 0.709 and relatively low positive ε_{Nd} values (+0.39 - +1.06). These data indicate that the Lipt granites have old crustal materials and presumably mantle-derived materials. Their Nd model ages are mostly in the range of 0.98 and 1.3 Ga suggesting that the old crustal component is of Middle Proterozoic age.

5. The Lipt granite pluton has remarkably high average concentrations of granitophile elements like Cs, Sn, Nb, Ta, Y, and Rb, which are similar to those of plumasitic specialized granites in the Arabian Shield. These high concentration levels of granitophile elements make it possible to consider the Lipt albite granite as mineralized granites
6. Fractional crystallization plays a significant role in the evolution of the Lipt granite pluton. Fluorine complexing and fluid fractionation paly a major role during the final stages of evolution. The fluid fractionation is the main process of evolution of the albite granite which led also to associating greisenization.

ACKNOWLEDGMENTS

The authors are greatly indebted to Dr. A. Moghazi, Alexandria Univ. for his valuable comments and for reading the manuscript. This research work is a part of the research project (AR-18-42) which has received financial support from the King Abdulaziz City for Sciences and Technology (KACST). Dr. R. Moufti, Dean of the Faculty of Earth Sciences is deeply appreciated for his encouragement and assistance during the progress of this work.

REFERENCES

Allegre, C.J., Hart, S.R., and Minster, J.F. 1983. Chemical structure and evolution of the mantle and continents determined by inversion of Nd and Sr isotopic data, II, Numerical experiments and discussion. *Earth Planet. Sci. Lett.* 37, 191-213

Barsukov, V.L. 1957. The geochemistry of tin. *Geochemistry* 1, 41-52.

Bergantz, G.W, 1989. Underplating and partial melting: implications for melt generation and extraction. *Science* 245: 1093-1095.

Beyth, M., Stern, R.J., Altherr, R., Kroner, A. 1994. The late Precambrian Timna igneous complex, southern Israel: Evidence for comagmatic-type sanukitoid monzodiorite and alkali granite magma. *Lithos* 31: 103 - 124.

Bohrson, W.A. and Reid, M.R. 1997. Genesis of silicate peralkaline volcanic rocks in an ocean island setting by crustal melting and open system processes, Socorro Island, Mexico. *J. Petrol.* 38, 1137-1166.

Calvez, J.Y. and Kemp, J. 1982. Geochronological investigation of the Mahd Ad Dahab Quadrangle, Central Arabian Shield. *Saudi Arabian Ministry of Mineral Resources Tech. Rec. BRGM-TR-02-5*, 40 pp.

Calvez, J.Y., Pellaton, C., Alsac, C., and Tegyey, M. 1983. Geochronology and geochemistry of plutonic rocks in the Umm Laij and Jabal Buwanah areas. *Unpubl. Tept. Saudi Arabian Deputy Ministry for mineral Resources.*

Camp, V.E., 1984. Island arcs and their role in the evolution of the western Arabian Shield. *Geol. Soc. Am. Bull.* 95, 913–921.

Clarke, D.B., MacDonald, M.A., Reynolds, P.H., Longstaffe, F.G. 1993. Leucogranites from the Eastern Part of the South Mountain Batholith, Nova Scotia. *J Petrol* 34: 653-679

Cooper, J.A., Stacey, J.S., Stoeser, D.B. and Fleck, R.J. 1979. An evaluation of the zircon method of isotopic dating in the southern Arabian Craton. *Contrib. Mineral. Petrol.* 68. 429-439.

Creaser RA, Price, RC, Wormald RJ 1991. A-type granite revisited: assessement of residual source model. *Geology* 19: 163-166

Cuney M, Marignac C, Weisbrod A. 1992. The Beauvoir topaz-lepidolite albite granite (Massif Central France): The disseminated magmatic Sn-Li-Ta-Nb-Be mineralization. *Econ Geol* 87: 1766 - 1794.

De la Roche H, Leterrier J, Grandelaude P, Marchal M 1980. A classification of volcanic and plutonic rocks using R1R2-diagram and major-element analyses - its relationships with current nomenclature. *Chem Geol* 29: 183 - 210.

De Paolo, D.J. 1981. Trace elements and isotopic effects of combined wallrock assimilation and fractional crystallization. *Earth Planet. Sci. Lett.* 53, 189-202

Debon F, Lemmet M 1999 Evolution of Mg/Fe ratios in late Variscan plutonic rocks from external crystalline massifs of the Alps (France, Italy, Switzerland). *J Petrol* 40: 1151 - 1185.

Dingwell, D.B. 1988. The structures and properties of fluorine-rich magmas: A review of experimental studies. In Taylor RP, Strong DF (eds) Recent advances in the study of granite-related mineral deposits, *Can Instit Mineral Metallog, Montreal Quebec*, pp 1 - 12.

Dostal J, Chatterjee A.K. 1995. Origin of topaz-bearing and related peraluminous granites of the late Devonian Davis Lake pluton, Nova Scotia, Canada: Crystal versus fluid fractionation. *Chem Geol* 123: 67 - 88.

Du Bray, E.A. 1986. Specialized granitoids in the southeastern Arabian Shield- case history of a regional assessment. *J. Afr. Earth Sci.*, 4. 169-176.

Duyverman, H.J., Harris, N.B.W. and Hawkesworth, C.J. 1982. Nd and Sr isotope evidence from the Arabian Shield. *Earth Planet. Sci. Lett.* 59: 315-326.

Eby G.N. 1990. The A-type granitoids: a review of their occurrence and chemical characteristics and speculations on their petrogenesis. *Lithos* 26: 115 - 134.

Eby G.N. 1992. Chemical subdivisions of the A-type granitoids: petrogenesis and tectonic implications. *Geology* 20: 641 - 644.

El Bouseily, A.M. and El Sokkary, A.A. 1975. The relation between Rb, Ba and Sr in granitic rocks. *Chemical Geology* 16, 207-219.

Fleck, R.J., Greenwood, W.R., Hadley, D.G., Andersen, R.E., Schmidt, D.L., 1980. Age and evolution of the southern part of the Arabian Shield. *Instit. Appl. Geol. Jeddah Bull.* 3, 1-17.

Genna,A., Nehlig, P., Le Goff, E., Guerrot, C., Shanti, M .2002. Proterozoic tectonism of the Arabian Shield. *Precambrian Research* 117, 21–4

Gettings, M.E., Blank, H.R., Mooney, W.D. and Healey, J.H. 1986. Crustal structure of southwestern Saudi Arabia. *Jour. Geoph. Res.* 91: 6491 - 6512.

Greenwood, W.R., Jackson, R.O., Johnson, P.R., 1986. Geologic map of the Jabal Al Hasir quadrangle, sheet 19F, Kingdom of Saudi Arabia. *Saudi Arabian Deputy Ministry for Mineral Resources Geoscience Map GM 94C*, scale 1:250,000, with text, p. 31.

Greenwood, W.R., Stoeser, D.B., Fleck, R.J., and Stacey, J.S. 1982. Late Proterozoic island arc complexes and tectonic belts in the southern part of the Arabian Shield, Kingdom of Saudi Arabia. *Saudi Arabian Ministry of Mineral Resources*, open file Report USGS-OF-02-8,46 p.

Greiling R.O., Abdeen, M.M., Dardir, A.A., El Akhal, H., El Ramly, M.F., Kamal El Din, G.M., Osman, A.F., Rashwan, A.A., Rice, A.H.N., Sadek, M.F. 1994. A structural synthesis of the Proterozoic Arabian-Nubian Shield in Egypt. *Geol Rundsch* 83: 484 - 501.

Groves, D.I. 1972. The geochemical evolution of tin-bearing granites in the Blue Tier Batholith, Tasmania. *Econ. Geol* 67. 445–458.

Hadley, D.G., Schmidt, D.L., 1980. Sedimentary rocks and basins of the Arabian Shield and their evolution. *Instit. Appl. Geol. Jeddah Bull.* 3, 25-50.

Harris, N 1985. Alkaline complexes from the Arabian Shield. *J Afr Earth Sci* 3: 83 - 88.

Hassanen MA 1997. Post-collision, A-type granites of Homrit Waggat complex, Egypt: Petrological and geochemical constraints on its origin. *Precamb Res* 82: 211 - 236.

Heinrich, C.A. 1990. The geochemistry of tin (-tungsten) ore deposits. *Econ. Geol.* 85, 457-481

Higgins NC, Solomon M, Varne R 1985. The genesis of the Blue Tier Batholith, northeastern Tasmania, Australia. *Lithos* 18: 129 - 149.

Jackson, N.J. 1986. Petrogenesis and evolution of Arabian felsic plutonic rocks. *J African Earth Sci* 4: 47-59

Jackson, N.J., Ramsay, C.R., 1980. Time-space relationships of Upper Precambrian volcanic and sedimentary units in the Central Arabian Shield. *J. Geol. Soc. London* 137, 617–628.

Jacobsen, N.J. and Wasserburg, G.J. 1984. Sm-Nd isotopic evolution of chondrites and achondrites, II, *Earth Planet. Sci. Lett.* 67, 137-150.

King PL, White AJR, Chappell BW, Allen MC 1997. Characterization and origin of aluminous A-type granites from the Lechlan Fold Belt Southeastern Australia. *J Petrol* 38: 371 - 391.

Küster D., Harms U., 1998. Post-collisional potassic granitoids from the southern and northwestern parts of the Late Neoproterozoic East African Orogen: a review. *Lithos* 45: 177 - 195.

Landenberger B., Collins WJ., 1996. Derivation of A-type granites from dehydrated charnockitic lower crust: evidence from the Chaelundi complex Eastern Australia. *J Petrol* 37: 145 - 170.

Laval, M., Le Bel, L., 1986. Felsic plutonism in the Al Amar-Idsas area, Kingdom of Saudi Arabia. *J. Afr. Earth Sci.* 4, 87–98.

Ludwig, K.R., 1991. Isoplot, a plotting and regression program for radiogenic isotope data. *U.S. Geol. Surv.. Open-file Report* 39, 91-445.

Mackenzie DE, Black LP, Sun S-s 1988. Origin of alkali feldspar granites: an example from the Poimena Granite, northeastern Tasmania, Australia. *Geochim Cosmochim Acta* 52: 2507 - 2524.

Maniar PD, Piccoli PM 1989. Tectonic discrimination of granitoids. *Geol Soc Am Bull* 101: 635-643

Manning DAC 1981. The effect of fluorine on liquidus phase relationships in the system Qz-Ab-Or with excess water. *Contrib Mineral Petrol* 76: 206 - 215.

McIntyre, G.A., Brooks, C. Compston, W. and Turek, A. 1966. The statistical assessment of Rb-Sr isochrons. *J. Geophys. Res.* 71, 5459-5468.

Moody, J.B., Jenkins, J.E. and Meyer, D. 1985.. An experimental investigation of the albitization of plagioclase. *Can. Mineral.* 23, 583-596.

Nurmi PA, Haapala I 1986. The Proterozoic granitoids of Finland: Granite types, metallogeny and relation to crustal evolution. *Bull Geol Soc Finland* 58: 431 - 453.

Pallister, J.S., Stacey, J.S., Fischer, L.B., Premo, W.R., 1987. Arabian Shield ophiolites and Late Proterozoic microplate accretion. *Geology* 15, 320–323.

Pearce JA, Harris NBW, Tindle AG 1984. Trace element discrimination diagrams for the tectonic interpretation of granitic rocks. *J Petrol* 25: 956-983

Qhadi, T. 2003. Rare-metal bearing peralkaline granite in Um Al Birak area, Arabian Shield, KSA: Geochemical and Sr-Nd isotope study (in press).

Raimbault, L., Charoy, B., Cuney, M. and Pollard, P.J. 1991. Comparative geochemistry of Ta-bearing granites. In Pagel, M. and Leroy, J. (Eds): Source , transport and deposition of metals. Rotterdam, Balkema, 793-796.

Ramsay, C.R. 1986. Specialized felsic plutonic rocks of the Arabian Shield and their precursors. *J African Earth Sci* 4: 153 – 168.

Rogers JJW, Satterfield ME 1994. Fluids of anorogenic granites: A preliminary assessment. *Mineral Petrol* 50: 157 - 171.

Roobol, M.J., Ramsay, C.R., Jackson, N.J. and Darbyshire, D.P.F. 1983. Late Proterozoic lavas of the central Arabian Shield-Evolution of an ancient volcanic arc system. *J. Geol. Soc. London*, 140, 185-202.

Schwartz MO 1992. Geochemical criteria for distinguishing magmatic and metasomatic albite-enrichment in granitoids - examples fro the Ta-Li granitYichun (China) anf the Sn-W deposit Tikus (Indonesia). *Mineral Dep* 27: 101 - 108.

Shand S.J 1927. The eruptive rocks, 1st edition. *New York: John Wiley*, 488 pp.

Sheraton W and Black, L.P 1973. Geochemistry of mineralized granitic rocks of north-east Queenland. *J. Geoch. Explor.* 2: 331-348.

Stacey, J.S., Doe, B.R., Roberts, R.J., Delevaux, M.H., and Gramlich, J.W. 1980. A lead isotope study of mineraliization in the Saudi Arabian Shield. *Contrib.. Mineral. Petrol.* 74. 175-188.

Stacey, J.S., Hedge, C.E., 1984. Geochronologic and isotopic evidence for early Proterozoic crust in the eastern Arabian Shield. *Geology* 12, 310–313.

Stacey, S.J. and Stoeser, B.S., 1983. Distribution of oceanic and continental leads in the Arabian-Nubian Shield. *Contrib. Mineral. Petrol.* 84: 91-105.

Stern RJ 1994. Arc assembly and continental collision in the Neoproterozoic East African Orogen: Implications for the consolidation of Gondwanaland. *Ann Rev Earth Planet Sci* 22: 319-351.

Stern, R.J., 2002. Crustal evolution in the East African Orogen: a neodymium isotopic prospective. *J. Afr. Earth Sci.* 34, 109-117.

Stoeser, D.B., Stacey, J.S., Greenwood, W.R. and Fischer, L.B. 1984. U-Pb zircon geochronology of the southern part of the Nabitah mobile belt and Pan-African continental collision in the Saudi Arabian Shield. *Saudi Arabian Ministry of Mineral Resources Tech. Rec. USGS-TR*-04-5, 88 pp.

Sun, S. S., 1982. Chemical composition and origin of the earth primitive mantle. *Geochim. Cosmochim. Acta*, 46: 179-192.

Sun-S, McDonough WE 1989.. Chemical and isotopic systematics of oceanic basalts: implications for mantle composition and processes. In Saunders AD, Norry MJ (eds.) Magmatism in the oceanic basins. *Geol Soc Spec Publ* 42: 313 - 345.

Sylvester PJ. 1989. Post-collisional alkaline granites. *J Geol* 97: 261-280

Tischendorf, G. 1977. Geochemical and petrographic characteristics of silicic magmatic rocks associated with rare element mineralizations. In: Stemprok, M. and Burnet, L. (eds.), Mineralization associated with acid magmatism, vol. 2: 41 - 96. *Czechoslovakian Geologic Survey, Prague.*

Wedepohl, KH., 1971. Geochemistry: *New York, Holt, Rinehart, and Winston, Inc.* 231p.

Whalen JB, Currie KL, Chappell BW 1987. A-type granites: geochemical characteristics, discrimination and petrogenesis. *Contrib Mineral Petrol* 95: 407-419.

Wolf MB, Wyllie PJ 1994. Dehydration-melting of amphibolites at 10 kbar: the effects of temperature and time. *Contrib Mineral Petrol* 115: 369-383.